

Supporting Information for

**Competitive ^{13}C and ^{18}O Kinetic Isotope Effects of
 $\text{Re}(\text{bpy})(\text{CO})_3\text{Cl}$ -Catalyzed CO_2 Reduction**

Taylor Schneider and Alfredo M. Angeles-Boza *

Table of contents	Page #
Experimental Section	S-3
Figure S1: FT-IR spectrum of reaction mixture produced by $\text{Re}(\text{bpy})(\text{CO})_3\text{Cl}$ (1) and $\text{Na}(\text{Hg})$ in acetonitrile.	S-5
Figure S2: FT-IR spectrum of reaction mixture produced during the photocatalytic reduction of CO_2 by $\text{Re}(\text{bpy})(\text{CO})_3\text{Cl}$ (1).	S-6
Figure S3: Schematic diagram of apparatus used for the measurement of competitive ^{13}C and ^{18}O isotope effects	S-7
Computational methods	S-7
Calculation of EIEs	S-8
Calculated vibrational frequencies	S-9
References	S-11

Experimental Section

General Procedures. ^1H NMR spectra were recorded on a Bruker AVANCE III (400 MHz) system at ambient temperature and were referenced to residual solvent peaks. Elemental analyses were performed at Atlantic Microlab, Inc., in Norcross, GA.

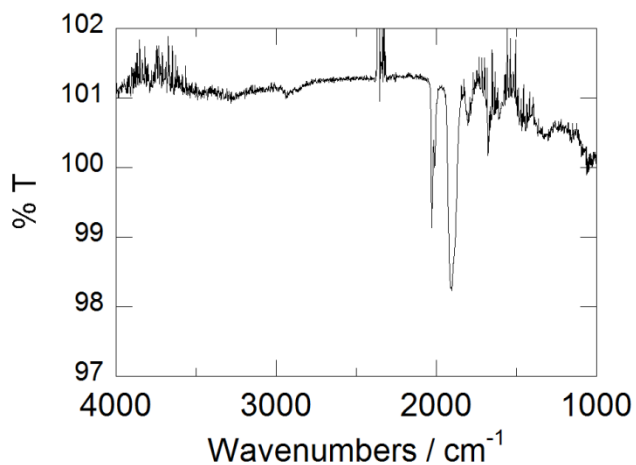
Materials. 2,2'-bipyridine, pentacarbonylchlororhenium (I), triethanolamine and Na(Hg) amalgam (5% Na by mass) were all purchased from Sigma-Aldrich and used as received. Solvents used in this work were purified by passing through a solvent purification system (Glass Contour).

Na(Hg)-Driven Reaction. Collection of gas for ^{13}C O and ^{18}O KIE analysis required the design of a special apparatus (Figure S2). A 0.5-2mM solution of (**1**) was added to the graduated solvent reservoir, and saturated with 1% CO_2 , backed with N_2 . The Na-Hg pellets were added to the lower chamber of the two-bulb component, and the apparatus, from the right of valve 1, onwards, was evacuated down to approximately 0.2 torr. Valves 3 and 4 were then closed, and a 20 mL portion of the catalyst solution was injected into the lower chamber by opening valve 1. The resulting reaction mixture was stirred for varying amounts of time (70 – 300 minutes). Once the reaction has run for the desired length of time, solvent trap A was immersed in a bath of liquid nitrogen. Valve 5 was closed, and valves 4 and 3 were opened, in that order. The reaction mixture would start to bubble as the sudden vacuum would cause it to outgas. A mixture of gases and CH_3CN solvent were collected in trap A. Valve 3 was closed after 2.5 minutes of constant outgassing from the reaction mixture. Valve 4 was left open for an additional five minutes. Valve 4 was then closed, and the liquid nitrogen was removed from trap A. The frozen solvent was given time to melt and collect at the bottom of the trap. Trap B was then immersed in liquid nitrogen, and valve 6 was closed. Trap A was then immersed in a cold bath of isopropanol/dry ice. This will keep the solvent frozen, but allow the gas to transfer over into trap B. Valve 5 was opened for ten minutes. Valves 4 and 6 were then also opened, to evacuate the N_2 and CO . The dry ice is cold enough that it keeps the CO_2 frozen, even at such low pressures. The same is true for the ability of the isopropanol/dry ice bath to retain the frozen solvent. Once the pressure of the system had dropped back down to 0.2 torr, valves 5 and 6 were closed. (NOTE: if there is enough solvent in trap A to completely block the system, then some solvent must first be transferred over to trap B, in the same manner by which solvent was transferred from the two-

bulb component to trap A. This solvent will then be allowed to thaw, and flow to the bottom of trap B before immersing traps A and B in isopropanol/dry ice and liquid nitrogen, respectively.) The liquid nitrogen bath over trap B was replaced with the isopropanol/dry ice bath. The bottom one-third of trap C was immersed in liquid nitrogen (approximately at marking *i*). Valves 8 and 9 were closed, and then valve 6 was opened. The pressure initially increased, but quickly declined as the CO₂ condensed in trap C. After ten minutes the pressure would have leveled off around 0.3 torr. The level of liquid nitrogen was then increased so that at least two-thirds of trap C was immersed (approximately marking *ii*). Valve 7 was closed. Valve 9 was opened to evacuate any uncondensed gasses, such as N₂ or CO. The liquid nitrogen is cold enough that the CO₂ in trap C will not evaporate, even at these low pressures. Valve 9 was closed, and the pressure, almost always around 0.2 torr, was recorded as P_{low}. The liquid nitrogen was removed from trap C, and the pressure increased as the CO₂ sublimated into gas. After a few minutes, the pressure leveled off, and this was recorded as P_{high}. The difference between P_{high} and P_{low} should be P_{CO₂}. (NOTE: The CO₂ pressure measured when no reaction occurs should be calculated based on the ideal gas law and the volume of this segment of the apparatus, and then measured experimentally. The measured pressure, P_{CO₂}, should be lower than the pressure of no reaction. If it is higher, then the other gases that might be present are either N₂, CO, or solvent vapor, or there is a leak.) After P_{CO₂} had been measured, the removable tube, labeled as trap D, was immersed in liquid nitrogen, and valve 8 was opened. The liquid nitrogen level sometimes needs to be adjusted to encourage complete selection of CO₂. Once all CO₂ had been collected, the liquid nitrogen level was raised slightly, and valve 9 was opened briefly. Valve 8 was then closed, and a propane blow torch was used to seal the tube 10 cm up from the bottom. The liquid nitrogen was removed, and the torch was used to completely remove the 10 cm segment from the rest of the apparatus.

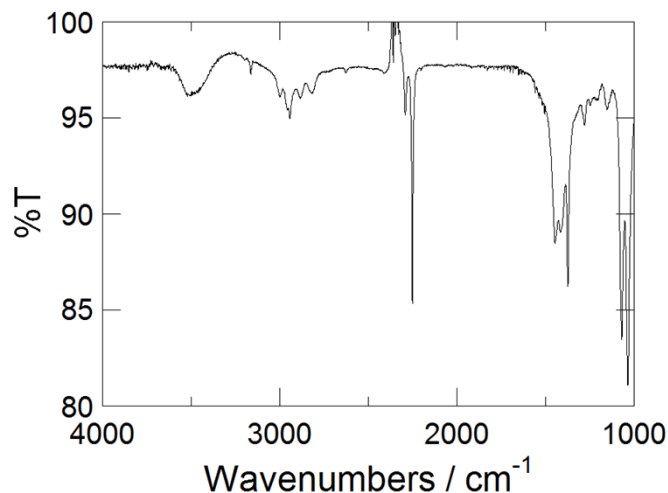
Formation of oxalate, carbonate and formate was not observed during these reactions. The oxalate formation was monitored using a commercial oxalate kit from Trinity Biotech (591D-1KT). The Na(Hg) pellets were first removed from the reaction flask under inert atmosphere. The remaining solution was rotary evaporated and the remaining solid was suspended in water (5 mL). The protocol detailed in the kit was then followed. We did not see evidence of oxalate, carbonate and formate formation through FT-IR (Figure S1).¹

Figure S1: FT-IR spectrum of reaction mixture produced by $\text{Re}(\text{bpy})(\text{CO})_3\text{Cl}$ (**1**) and $\text{Na}(\text{Hg})$ in acetonitrile.



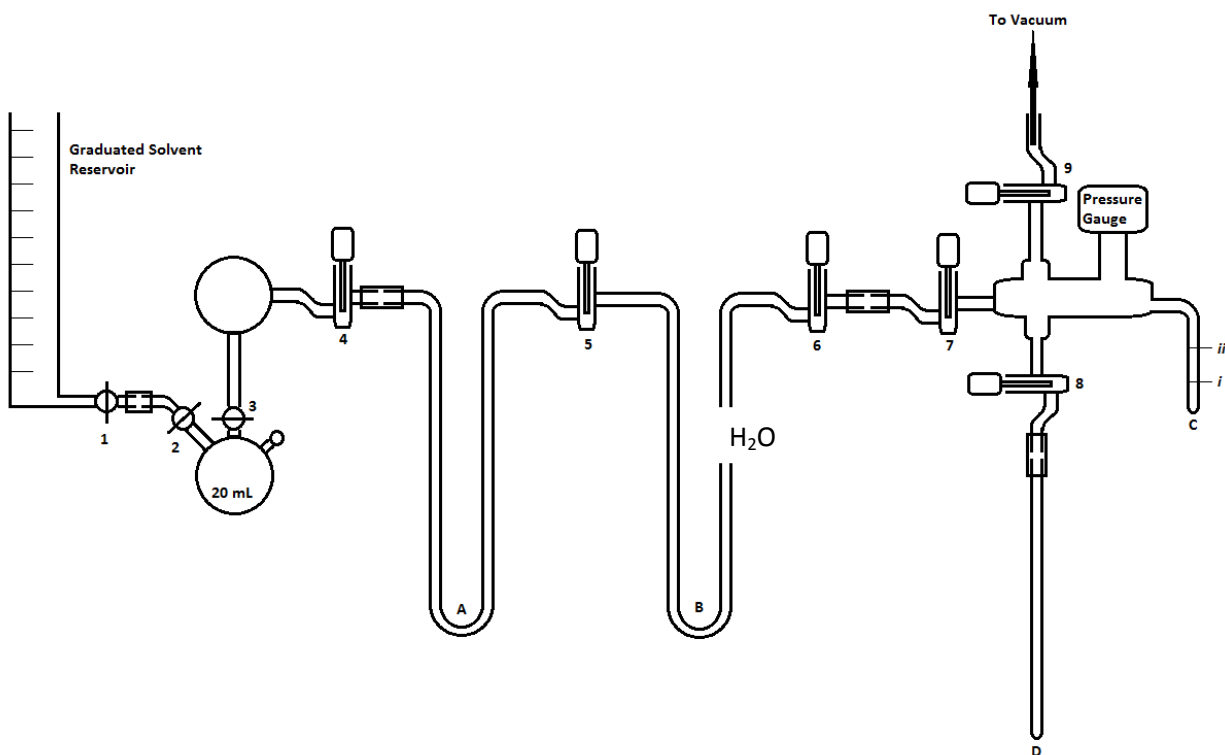
Photochemistry. The photochemistry was performed in a solution that was five parts acetonitrile to one part triethanolamine (TEOA). The catalyst concentration was ranged from 0.5 mM to 2 mM, depending on the individual reactions. The same reaction vessel used in the $\text{Na}(\text{Hg})$ -driven reductions was used here. A 20mL portion of the solution was introduced to the lower portion of the bulb after saturating the solution with the 1% CO_2 gas mixture. The vessel was then removed from the manifold setup, and photolysis initiated using a 150-W Hg/Xe lamp equipped with a dichroic mirror and a band-pass filter (350 - 450 nm). The reaction times for the photochemical experiments were much longer than those involving the $\text{Na}(\text{Hg})$ amalgam, and were between 16 and 72 hours to obtain a range of CO_2 conversions. Once these reactions were performed, the reaction vessel was re-attached to the KIE manifold, and the remaining CO_2 was collected in a method identical to that described above.

Figure S2: FT-IR spectrum of reaction mixture produced during the photocatalytic reduction of CO₂ by Re(bpy)(CO)₃Cl (**1**). Spectrum is dominated by the TEOA peaks.



Synthesis. Re(bpy)(CO)₃Cl was prepared according to previously reported methods. Three different batches were prepared for the current experiments. Briefly, in a 100 mL round bottom flask, Re(CO)₅Cl (0.502g, 1.35 mmol), 2,2'-bipyridine (0.0211g, 1.35 mmol) and toluene (50 mL) were added together and the resultant reaction mixture was heated under refluxing conditions. After 5 hours, the product was vacuum filtered, and rinsed with cold toluene. Yield 0.40 g (65 %). ¹H NMR (δ, 400 MHz, DMSO-*d*₆): 9.02 (d, 1H), 8.77 (d, 1H), 8.34(t, 1H), 7.76(t, 1H). FT-IR (acetonitrile): 2022 (vs), 1917 (s), 1900 (s).² Anal. Found for C₁₃H₈N₂O₃ClRe: C, 40.30; H, 2.05; N, 5.76. Calcd. C, 40.47; H, 1.75; N, 6.06.

Figure S3. Schematic diagram of apparatus used for the measurement of competitive ^{13}C and ^{18}O isotope effects. Valves 1-3 are ground glass stopcocks coated in APIEZON® H-Grease to provide an adequate seal at high vacuum. Valves 4-9 are Teflon screw-cap valves. The various segments are connected by Swagelok® Ultra-Torr straight fittings.



Computational Methods.

All geometries were fully-optimized at three levels of DFT. One approach employed the previously validated *mPW* functional, 6-311G(d) basis set for O and C, and 6-31G for H. Calculations were carried out using the Gaussian09 package.³ The second approach employed the BP86 functional, along with the 6-311G(d) basis set for the O and C atoms, and the 6-31G basis set for the H atom. The third approach used the B3LYP functional with 6-311G(d) basis set for O and C, and 6-31G for H. The vibrations were calculated after all the geometries were fully optimized using the *mPWPW91*, BP86 and B3LYP functionals, and 6-311G(d) basis set for O and C, and 6-31G basis set for H.

Calculations of ^{18}O EIEs

The complete set of vibrational frequencies was implemented for the initial (A) and final (B) states per the Redlich-Teller product rule, using the generic isotope exchange equation $A + B^* \rightarrow A^* + B$, where the asterisk designated the site of the heavy isotope. A is the initial reactant and B is the product, both with $3N-6$ stable modes, where N is the number of atoms. The product with $3N-6$ vibrations was used to calculate ^{18}O EIEs, where additional terms include h (Planck's constant), k (Boltzmann's constant) and T is temperature.

$$(S-1) \quad {}^{18}\text{O EIE} = ZPE \times EXC \times MMI$$

$$(S-2) \quad ZPE = \frac{\left[\prod_j^{3N-6} \frac{\exp(h\nu_j^{B^*}/(2kT))}{\exp(h\nu_j^B/(2kT))} \right]}{\left[\prod_i^{3N-6} \frac{\exp(h\nu_i^{A^*}/(2kT))}{\exp(h\nu_i^A/(2kT))} \right]}$$

$$(S-3) \quad EXC = \frac{\left[\prod_j^{3N-6} \frac{1 - \exp\{-h\nu_j^{B^*}/(kT)\}}{1 - \exp\{-h\nu_j^B/(kT)\}} \right]}{\left[\prod_i^{3N-6} \frac{1 - \exp\{-h\nu_i^{A^*}/(kT)\}}{1 - \exp\{-h\nu_i^A/(kT)\}} \right]}$$

$$(S-4) \quad MMI = \frac{\prod_j^{3N-6} (\nu_j^B / \nu_j^{B^*})}{\prod_i^{3N-6} (\nu_i^A / \nu_i^{A^*})}$$

Calculated Vibrational Frequencies used for the calculation of EIEs

CO₂ (B3LYP)

12, 16, 16	13, 16, 16	12,16,18
666.4978	647.5285	661.4171
1375.6153	1375.6155	1335.8974
2436.0748	2366.7412	2417.9884

CO₂ (mPWPW91)

12, 16, 16	13, 16, 16	12,16,18
639.996	621.7809	635.1172
1324.725	1324.7252	1286.4877
2383.0274	2315.2036	2365.3141

CO₂ (BP86)

12, 16, 16	13, 16, 16	12,16,18
637.94	619.7835	633.0769
1318.4081	1318.4083	1280.353
2371.4039	2303.911	2353.7772

CO₂⁻ (B3LYP)

12, 16, 16	13, 16, 16	12,16,18
740.676	730.4338	726.5864
1330.6272	1310.8833	1306.8291
1689.4177	1643.6106	1675.772

CO₂⁻ (mPWPW91)

12, 16, 16	13, 16, 16	12,16,18
711.1664	701.3869	697.6004
1280.5233	1261.4247	1257.718
1641.054	1596.5933	1627.737

CO₂⁻ (BP86)

12, 16, 16	13, 16, 16	12,16,18
708.2547	698.5356	694.7283
1273.1744	1254.1489	1250.5257
1629.82	1585.6685	1616.5945

H₂O (B3LYP)

16	18
1691.9171	1684.7397
3733.4812	3725.9513
3853.4465	3837.4963

H₂O (*m*PWPW91)

16	18
1672.7234	1665.6595
3648.8881	3641.4586
3774.3366	3758.8977

H₂O (BP86)

16	18
1666.1381	1659.0897
3631.9207	3624.5526
3758.2484	3742.8681

CO (B3LYP)

12, 16	13, 16	12, 18
2220.5599	2171.0604	2166.9172

CO (mPWPW91)

12, 16	13, 16	12, 18
2134.1072	2086.5349	2082.553

CO (BP86)

12, 16	13, 16	12, 18
2124.681	2077.3188	2073.3545

References

1. Spectrum was compared to the FT-IR spectra compiled by NIST. Oxalate: <http://webbook.nist.gov/cgi/cbook.cgi?ID=C62760&Type=IR-SPEC&Index=2#IR-SPEC>; carbonate: <http://webbook.nist.gov/cgi/cbook.cgi?ID=C497198&Type=IR-SPEC&Index=1#IR-SPEC>; and formate: <http://webbook.nist.gov/cgi/cbook.cgi?Formula=HCOONa&NoIon=on&Units=SI&cIR=on>.
2. Values agree with those reported for $\text{Re}(\text{bpy})(\text{CO})_3\text{Cl}$. See for example: Smieja, J. M.; Kubiak, C. P. *Inorg. Chem.* **2010**, *49*, 9283-9289.
3. Gaussian 03, Revision C.02, Frisch, M. J.; Trucks, G. W.; Schlegel, H. B.; Scuseria, G. E.; Robb, M. A.; Cheeseman, J. R.; Montgomery, Jr., J. A.; Vreven, T.; Kudin, K. N.; Burant, J. C.; Millam, J. M.; Iyengar, S. S.; Tomasi, J.; Barone, V.; Mennucci, B.; Cossi, M.; Scalmani, G.; Rega, N.; Petersson, G. A.; Nakatsuji, H.; Hada, M.; Ehara, M.; Toyota, K.; Fukuda, R.; Hasegawa, J.; Ishida, M.; Nakajima, T.; Honda, Y.; Kitao, O.; Nakai, H.; Klene, M.; Li, X.; Knox, J. E.; Hratchian, H. P.; Cross, J. B.; Adamo, C.; Jaramillo, J.; Gomperts, R.; Stratmann, R. E.; Yazyev, O.; Austin, A. J.; Cammi, R.; Pomelli, C.; Ochterski, J. W.; Ayala, P. Y.; Morokuma, K.; Voth, G. A.; Salvador, P.;

Dannenberg, J. J.; Zakrzewski, V. G.; Dapprich, S.; Daniels, A. D.; Strain, M. C.; Farkas, O.; Malick, D. K.; Rabuck, A. D.; Raghavachari, K.; Foresman, J. B.; Ortiz, J. V.; Cui, Q.; Baboul, A. G.; Clifford, S.; Cioslowski, J.; Stefanov, B. B.; Liu, G.; Liashenko, A.; Piskorz, P.; Komaromi, I.; Martin, R. L.; Fox, D. J.; Keith, T.; Al-Laham, M. A.; Peng, C. Y.; Nanayakkara, A.; Challacombe, M.; Gill, P. M. W.; Johnson, B.; Chen, W.; Wong, M. W.; Gonzalez, C.; Pople, J. A. Gaussian, Inc., Wallingford CT, 2004